Feedback Rate Optimization in Receiver-Coordinated Distributed Transmit Beamforming for Wireless Power Transfer

Rui Wang, Radu David, and D. Richard Brown III
Dept. of Electrical and Computer Eng.
Worcester Polytechnic Institute
100 Institute Rd, Worcester, MA 01609
Email: {rwang,radud,drb}@wpi.edu

***Abstract*—This paper considers the combination of receiver-coordinated distributed transmit beamforming with wireless power transfer in a narrowband wireless communication system. A single receiver measures the channel states of two or more independent transmit nodes and provides feedback to the transmitters to facilitate beamforming and passband signal alignment at the receiver. The receive node is equipped with energy harvesting and storage devices which can harvest and store the beamforming energy for future utilization. Since feedback improves the beamforming gain but requires the receiver to expend energy, there is an inherent tradeoff between the feedback rate and the efficiency of the energy harvesting at the receiver. This paper analyzes the optimal feedback rate to maximize the amount of energy harvested by the receive node per unit of time. Analysis shows that there always exists a unique optimal feedback rate for the system. Numerical results are also provided to confirm the analysis and demonstrate the effect of the feedback rate on the mean energy harvesting rate.**

***Index Terms*—distributed beamforming, wireless power transfer, synchronization, channel state feedback**

I. Introduction

Distributed transmit beamforming is a technique in which two or more separate transmitters simultaneously transmit a common message and control the phase of their passband transmissions so that the signals constructively combine at an intended destination [1]–[6]. Distributed coherent transmission techniques offer the potential gains of conventional antenna arrays to wireless communication systems composed of multiple single-antenna transmitters with independent local clocks. In systems with M transmit nodes and per-node power constraints, fully-coherent distributed transmit beamforming results in M^2 power gains on target with respect to single-node transmission and a factor of M power gain on target with respect to incoherent transmission [7], [8].

Recently, wireless power transfer (WPT) using radio frequency signals [9]–[15] is attracting attention as a viable approach to prolong the lifetime of battery powered devices in wireless networks due to the fact that sometimes replacing or recharging batteries may be inconvenient (e.g., for a sensor network with a large number of distributed sensor nodes), dangerous (e.g., for devices positioned in toxic environments), or even impossible (e.g., for the medical sensors implanted inside human bodies).

To the best of our knowledge, all of the previous literature on distributed transmit beamforming has focused on the *communication* problem. Similarly, the wireless power transfer literature has focused on the use of single-antenna transceivers or conventional (centralized) antenna arrays. There have been no studies on the potential use of distributed transmit beamforming for wireless power transfer.

This paper considers the use of distributed transmit beamforming for wireless power transfer assuming each node in the system has an independent local oscillator and that no exogenous synchronization signals are present. The receive node is equipped with energy harvesting and storage devices and provides feedback to the transmit nodes to facilitate beamforming and passband signal alignment. Note that there is an inherent tradeoff in the feedback rate and the beamforming gain. With no feedback, the receiver only achieves incoherent power from the transmit nodes. As the feedback rate increases, the transmit nodes are able to achieve beamforming gains closer to ideal. These gains have diminishing return with increasing feedback rate, however. Hence, the goal of the receive node is to provide feedback at a rate that maximizes the amount of energy harvested from the distributed transmit array per unit of time.

In this paper, we develop a model to analyze the performance of distributed transmit beamforming for wireless power transfer in the receiver-coordinated scenario. We formulate an optimization problem to find the optimal feedback rate to maximize the *mean energy harvesting rate* (MEHR) at the receive node. The MEHR is defined as the net amount of energy harvested by the receive node per unit of time. A simple lower bound for the MEHR is derived. Based on this lower bound, the analysis shows that there always exists a unique optimal feedback rate provided the system parameters satisfy certain mild constraints. Numerical results are also provided to confirm the analysis and to demonstrate the performance of energy harvesting with distributed transmit beamforming and

This work was supported by the National Science Foundation awards CCF-1302104 and CCF-1319458.

feedback rate optimization.

II. System Model

We consider the wireless communication system shown in Fig. 1 with M transmit nodes and one receive node. Each node in the system is assumed to possess an independent local oscillator and a single isotropic antenna. The channels from the transmit nodes to the receive nodes are called the "forward link" and the channels from the receive node to the transmit nodes are called the "reverse link". We assume a scenario where the receive node periodically estimates the forward link channels and provides feedback on the reverse link to facilitate coherent transmission and passband signal alignment in the forward link. Forward link and reverse link transmissions are assumed to be on different frequencies, hence channel reciprocity techniques can not be used to estimate the forward link channels from reverse link measurements.

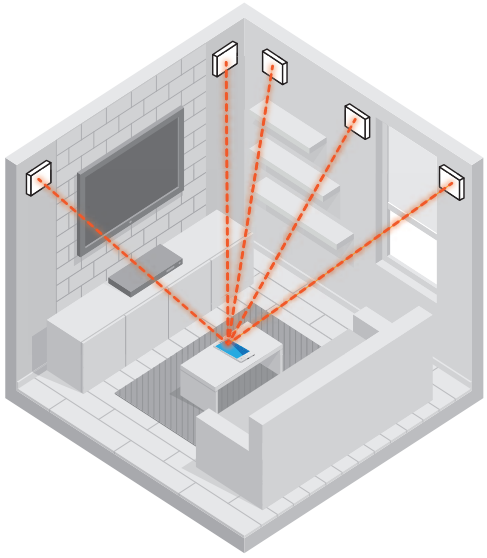

Fig. 1. System model example with M=5 transmit nodes.

We assume the receiver-coordinated protocol as described in [5] and illustrated in Fig. 2. Forward link transmissions are divided into measurement and beamforming epochs, repeating periodically with period T_f. The time duration for measurement and beamforming epochs are denoted as T_m and T_b, respectively, with $T_f = T_m + T_b$. During the measurement epoch, the receiver measures the forward link channels for subsequent feedback to facilitate distributed coherent transmission. During the beamforming epoch, the transmit nodes use the feedback to calculate an appropriate beamforming vector for distributed coherent transmission to the receiver. Without feedback from the receiver, the transmit nodes can only transmit incoherently to the receiver and the amount of power observed at the receiver can be significantly less than the power achieved even with approximate beamforming.

During the measurement epoch, the receive node estimates the phase of the received signal from each transmit node. We assume that the duration of the measurement epoch T_m is

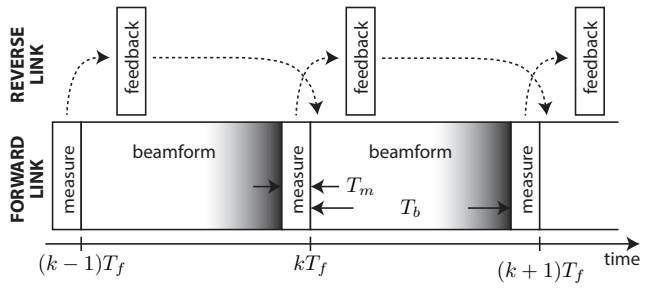

Fig. 2. Receiver-coordinated distributed transmit beamforming.

linear with respect to the number of transmit nodes, i.e., $T_m = MT_0$, where T_0 is a fixed measurement duration for a single transmit node.

After measuring each channel, the receiver feeds back the measurements to the transmit nodes so the transmit nodes can track their channels, generate channel predictions, and generate transmit beamforming coefficients. It is assumed that the receive node sends N bits of information for each channel measurement and, hence, the receive node provides MN total bits of feedback in each frame. To ensure that the transmit nodes can correctly decode the feedback, the total energy used for sending feedback, denoted as E_f, is assumed to be fixed and larger than some minimum decoding threshold E_t, i.e., $E_f \geq E_t$. Section V provides an example of a minimum decoding threshold link-budget calculation based on the distance between the transmit nodes and the receive node, the number of bits used for feedback, and the feedback data rate. Over the beamforming epoch, each transmit node uses its state predictions to compute a corrected transmit phase so that the phase offset of the passband signals after propagation to the receive node is nominally zero.

The receive node is equipped with energy harvesting and storage devices which can harvest and store the energy received wirelessly from the transmit nodes for future utilization. The net amount of energy harvested by the receive node in each period is the amount of energy received wirelessly from the distributed transmit array minus the amount of energy used for feedback. We denote the beamforming power at the receive node at time t as $J(t)$ and note that $J(t)$ is a stochastic process since the channel estimates are noisy. We further denote the ensemble averaged beamforming power as $\bar{J}(t) = \mathbb{E}[J(t)]$. The total average beamforming energy obtained by the receive node during the k^{th} period of the protocol is then

$$E_b = \eta \int_{kT_f}^{kT_f+T_b} \bar{J}(t)\, dt \tag{1}$$

where $kT_f, k \geq 0$ is the start of the beamforming epoch (after k measurement periods) and $\eta \in (0,1)$ is the harvesting efficiency. Thus, after subtracting the energy for the feedback, the average amount of energy harvested by the receive node over one period is $E_h = E_b - E_f$. The mean energy harvesting rate (MEHR) is defined as

$$\mathsf{MEHR} = \frac{E_h}{T_f} = \frac{E_b - E_f}{T_f}. \tag{2}$$

Our goal is to find the optimal feedback period T_f (feedback rate $\frac{1}{T_f}$) to maximize the MEHR.

III. Tracking Model

Each node in the system is assumed to have an independent local oscillator. These local oscillators behave stochastically, causing phase offset variations in each effective channel from transmit node to the receive node. To characterize the oscillator dynamics of each node in the system, we consider a simple one-state model. Adopting the convention that the receive node is node 0, we denote $\phi_i[k] = \phi_i(kT)$ as the carrier phase offset in radians at node $i \in \{0, \ldots, M\}$ with respect to an ideal carrier phase reference at time $t = kT$, where T is the sampling period of the discrete-time model. We assume the carrier phase offset dynamics at each node are governed by

$$\phi_i[k+1] = \phi_i[k] + u_i[k] \tag{3}$$

where $u_i[k] \overset{\text{i.i.d.}}{\sim} \mathcal{N}(0, Q_i(T))$ is the process noise which is assumed to be spatially and temporally i.i.d.. The variance of the discrete-time process noise is derived from a continuous-time model in [16] and can be expressed as

$$Q_i(T) = \omega_F^2 \left(p_i T + q_i \frac{T^3}{3} \right) \tag{4}$$

where ω_F is the forward link common carrier frequency in radians per second and p_i (units of seconds) and q_i (units of Hertz) are the process noise parameters corresponding to white frequency noise and random walk frequency noise, respectively. We assume that all of the oscillators have the same process noise parameters, i.e., $p_i \equiv p$ and $q_i \equiv q$ for all $i \in \{0, \ldots, M\}$ for the remainder of the paper.

We denote the phase of the i^{th} forward link propagation channel as ψ_i and assume this quantity to be time invariant. The *pairwise offset* between the i^{th} transmit node and the receive node after propagation is defined as $\delta_i[k] = \phi_i[k] + \psi_i - \phi_0[k]$ and is governed by the state update

$$\begin{aligned} \delta_i[k+1] &= \delta_i[k] + u_i[k] - u_0[k] \\ &= \delta_i[k] + \boldsymbol{G}\boldsymbol{u}_i[k] \end{aligned} \tag{5}$$

where $\boldsymbol{G} = [1, -1]$ and $\boldsymbol{u}_i[k] = [u_i[k] \;\; u_0[k]]^\top$ for $i = 1, \ldots, M$. Since the ideal carrier phase reference and the propagation phases $\{\psi_i\}$ are unknown, the receiver is only able to observe these pairwise phase offsets. The observation of the i^{th} forward link channel at the receiver is then

$$y_i[k] = \delta_i[k] + v_i[k] \tag{6}$$

where $v_i[k] \overset{\text{i.i.d.}}{\sim} \mathcal{N}(0, R)$ is the measurement noise which is assumed to be spatially and temporally i.i.d..

The noisy observations in (6) are transmitted over the reverse link from the receiver to the transmit nodes. Each transmit node applies these observations to a Kalman filter to generate state estimates $\hat{\delta}_i[k|k]$ and state predictions $\hat{\delta}_i[k+L|k]$ for the next beamforming epoch. The value of L is a function of the feedback latency, i.e., the time between the observation and the start of the beamforming epoch in which the observation is used, the duration of the beamforming epoch T_b, and the sampling period T. Over the beamforming epoch, each transmit node uses its state prediction vector to compute a *corrected* transmit phase so that the phase offset at the receive node after propagation is nominally zero.

It can be shown that the system described in (5) and (6) is completely observable and completely controllable. Thus, the Kalman filter steady-state prediction variance at time T_f, which is denoted as $P(T_f)$, is a unique positive solution of the following scalar discrete-time algebraic Riccati equation (DARE) [17]

$$\frac{P(T_f)^2}{P(T_f) + R} = Q(T_f) \tag{7}$$

where

$$Q(T_f) = \boldsymbol{G}\text{cov}\{\boldsymbol{u}_i[k]\}\boldsymbol{G}^\top = AT_f + B\frac{T_f^3}{3} \tag{8}$$

with $A = 2\omega_F^2 p$ and $B = 2\omega_F^2 q$. Note that $P(T_f) > 0$ corresponds to the variance of the steady-state Kalman filter predictions just prior to an observation. The Kalman filter steady-state estimation variance immediately after receiving an observation can be expressed as

$$S(T_f) = P(T_f) - \frac{P(T_f)^2}{P(T_f) + R}. \tag{9}$$

The Kalman filter steady-state prediction variance at any elapsed time $t > 0$ from an observation at time kT_f follows as

$$\sigma_\phi^2(kT_f + t) = S(T_f) + Q(t). \tag{10}$$

Assuming identical channel gains of g and a unit total transmit power constraint, the mean beamforming power at any time τ in a beamforming epoch can be expressed as [5]

$$\bar{J}(\tau) = g^2 \left(M e^{-\sigma_\phi^2(\tau)} + \left(1 - e^{-\sigma_\phi^2(\tau)} \right) \right) \tag{11}$$

where $\sigma_\phi^2(\tau)$ is the variance of the phase prediction of the i^{th} transmit node at time τ. Observe that, in light of (10) and (11), the mean beamforming power $\bar{J}(\tau) = \bar{J}(kT_f + t)$ is a function of the feedback period T_f and the elapsed time from the k^{th} observation t. Therefore, to emphasize this relationship, we replace $\bar{J}(\tau)$ with $\bar{J}(T_f, t)$ for the remainder of the paper.

IV. Analysis

This section analyzes the MEHR maximization problem. We show that, using a lower bound expression for the MEHR, there always exists a unique global optimal feedback rate to maximize the MEHR lower bound. First, we provide an expression for the unique positive steady-state estimation variance $S(T_f)$ in the following Lemma.

Lemma 1. *Given $R > 0$ and $Q(T_f) > 0$, the unique positive steady-state estimation variance $S(T_f)$ is*

$$S(T_f) = \frac{-Q(T_f) + \sqrt{Q(T_f)^2 + 4RQ(T_f)}}{2}. \tag{12}$$

Proof: Note that (7) is quadratic in $P(T_f)$ and has two solutions. Since $R > 0$ and $Q(T_f) > 0$, the unique positive solution is

$$P(T_f) = \frac{Q(T_f) + \sqrt{Q(T_f)^2 + 4RQ(T_f)}}{2}. \quad (13)$$

From (9), it follows that

$$S(T_f) = \frac{-Q(T_f) + \sqrt{Q(T_f)^2 + 4RQ(T_f)}}{2} \quad (14)$$

which shows the desired result. ∎

The following Lemma provides an upper bound for the steady-state estimation variance $S(T_f)$.

Lemma 2. *Given $R > 0$, $P(T_f) > 0$, and $S(T_f)$ according to (9), we have*

$$0 < S(T_f) < R.$$

Proof: Since $R > 0$, it follows that

$$\begin{aligned}
&\Leftrightarrow R^2 > 0 \\
&\Leftrightarrow R^2 + P(T_f)R > P(T_f)R + P^2(T_f) - P^2(T_f) > 0 \\
&\Leftrightarrow R(P(T_f) + R) > P(T_f)(P(T_f) + R) - P^2(T_f) > 0 \\
&\Leftrightarrow R > P(T_f) - \frac{P^2(T_f)}{P(T_f) + R} > 0 \\
&\Leftrightarrow R > S(T_f) > 0
\end{aligned}$$

where the last inequality follows from (9). ∎

Lemma 2 and (10) imply that the steady-state phase prediction variance is upper bounded as

$$\sigma_\phi^2(kT_f + t) < R + Q(t).$$

Assuming zero feedback latency, this result in combination with (11) further implies that

$$\begin{aligned}
\bar{J}(T_f, t) > \check{J}(T_f, t) &= g^2 \left(\frac{M-1}{e^R} e^{-Q(t-kT_f)} + 1 \right) \\
&= g^2 \left(Ce^{-Q(t-kT_f)} + 1 \right). \quad (15)
\end{aligned}$$

for $C = (M-1)e^{-R}$, $t \in [kT_f, kT_f + T_b]$, and k sufficiently large so that the Kalman filter is in steady-state. We will show that this lower bound tends to be a close approximation for $\bar{J}(T_f, t)$ in Section V.

The following theorem establishes the existence and uniqueness of the solution of the MEHR maximization problem using the lower bound (15). For notational convenience, we define

$$F(x) = \int_0^x e^{-Q(t)} dt - e^{-Q(x)}(x + T_m). \quad (16)$$

Theorem 1. *Using the lower bound $\check{J}(T_f, t)$, if*

$$\frac{1}{C} \left(T_m + \frac{E_f}{\eta g^2} \right) \leq \lim_{T_b \to \infty} \int_0^{T_b} e^{-Q(t)} \, dt \quad (17)$$

then there exists a unique optimal feedback period $T_f^\star = T_m + T_b^\star$ satisfying

$$F(T_b^\star) = \frac{1}{C} \left(T_m + \frac{E_f}{\eta g^2} \right). \quad (18)$$

A proof of this theorem is provided in the Appendix. Intuitively, the condition in (17) ensures that the receive node can harvest enough energy so that the MEHR can be positive. If this condition is not satisfied, the optimal strategy is to provide no feedback and simply harvest the incoherent power.

The following Corollary provides an expression for the maximum MEHR.

Corollary 1. *Using the lower bound $\check{J}(T_f, t)$, the maximum MEHR is*

$$\mathsf{MEHR}^\star = \eta g^2 \left(Ce^{-Q(T_b^\star)} + 1 \right) \quad (19)$$

where $T_b^\star$ is the unique solution of (18).

Proof: Using the lower bound $\check{J}(T_f, t)$ in (15), the maximum MEHR can be written as

$$\begin{aligned}
\mathsf{MEHR}^\star &= \frac{1}{T_f^\star} \left(\eta g^2 \int_{kT_f^\star}^{kT_f^\star + T_b^\star} \left(Ce^{-Q(t-kT_f^\star)} + 1 \right) dt - E_f \right) \\
&= \frac{1}{T_f^\star} \left(\eta g^2 \int_0^{T_b^\star} Ce^{-Q(t)} \, dt + \eta g^2 T_b^\star - E_f \right) \quad (20)
\end{aligned}$$

From (16) and (18), it follows that

$$\begin{aligned}
\eta g^2 \int_0^{T_b^\star} Ce^{-Q(t)} \, dt &= \eta g^2 C \left(F(T_b^\star) + e^{-Q(T_b^\star)}(T_b^\star + T_m) \right) \\
&= \eta g^2 T_m + E_f + \eta g^2 Ce^{-Q(T_b^\star)} T_f^\star \quad (21)
\end{aligned}$$

Plugging (21) into (20), we obtain the desired result. ∎

V. Numerical Results

This section provides numerical results to confirm the analysis in Section IV and to demonstrate the potential for distributed transmit beamforming for wireless power transfer. Table I lists the parameters in the simulations. The process noise parameters p and q in Table I are chosen based on the Rakon RFPO45 oven-controlled oscillator datasheet [18].

TABLE I
Parameters for numerical results.

Parameter	Value	Units	Meaning
p	2.31×10^{-21}	sec	oscillator short-term stability
q	6.80×10^{-23}	Hertz	oscillator long-term stability
ω_F	$2\pi \cdot 1 \times 10^9$	rad/sec	forward link carrier frequency
ω_R	$2\pi \cdot 2.4 \times 10^9$	rad/sec	reverse link carrier frequency
B_R	10×10^6	Hertz	reverse link bandwidth
R_R	6	Mbps	reverse link data rate
T_0	5×10^{-2}	sec	duration of measurement for single transmit node
N	32		number of bits per channel measurement
G	0	dBi	antenna gains
d	3	meters	link distance
α	3		path loss exponent
R	$\left(\frac{10 \cdot 2\pi}{360}\right)^2$	rad^2	measurement noise
η	0.50		energy harvesting efficiency

We first calculate the minimum decoding threshold. Assuming a thermal noise floor of -174 dBm, we can calculate the power of the additive white Gaussian noise at each transmit node as $-174 + 10\log_{10} B_R = -104$ dBm. We assume the transmitters require 3dB SNR to decode the feedback. Hence, the received signal power at each transmit node should be at least $-104 + 3 = -101$ dBm. The reverse link path loss can be calculated as $10\log_{10}\left(\frac{4\pi d\omega_R}{2\pi c}\right)^{\alpha} = 74.38$ dB, where $c = 3\times 10^8$ m/sec is the velocity of light. Thus, the minimum transmit power for a receive node sending feedback should be $-101 + 74.38 - G = -26.62$ dBm or 2.18×10^{-6} Watts. The total time to send feedback to one transmit node is $\frac{N}{R_R} = 5.33\times 10^{-6}$ sec. Hence, the minimum total energy for feedback to M transmit nodes is

$$\begin{aligned} E_t &= M\cdot\left(2.18\times 10^{-6}\right)\text{ Watts}\cdot\left(5.33\times 10^{-6}\right)\text{ sec} \\ &= M\cdot 1.16\times 10^{-11}\text{ Joules.} \end{aligned}$$

The numerical results in this section assume a total feedback energy of $E_f = M\cdot 2\times 10^{-11}$ Joules.

To obtain the forward link path loss g^2, we use the forward link carrier frequency ω_F to calculate $g^2 = \left(\frac{4\pi d\omega_F}{2\pi c}\right)^{-\alpha} = 5.04\times 10^{-7}$. This corresponds to approximately a 63 dB path loss in the forward link.

Figure 3 shows the lower bound for the MEHR by using (15) and the actual MEHR calculated with a numerical solver versus the feedback period for an $M = 10$ transmit node system. We observe that the lower bound of the MEHR in (15) is very close to the actual (numerically calculated) MEHR. The unique optimum feedback period $T_f^\star \approx 2.75$ sec is clearly evident in these results. Note that the MEHR is quite steep for $T_f < T_f^\star$. Even though the receiver enjoys a highly-coherent beam in this regime, increasing the feedback rate (decreasing T_f) only results in small gains in harvested energy and actually decreases the MEHR. When $T_f > T_f^\star$, the receiver is not providing enough feedback to achieve a level of coherency to maximize the MEHR. When T_f becomes very large, the MEHR approaches the non-coherent power level.

Figure 4 shows the optimal feedback rate $\frac{1}{T_f^\star}$ versus the number of transmit nodes M. This example shows that the optimal feedback rate decreases with the number of transmit nodes. This is caused both by the fact that $T_m = MT_0$ is increasing with M and the fact that $T_b^\star$ is increasing with M. Intuitively, as M becomes large, the energy cost of the feedback also becomes large and the receiver optimizes its MEHR by sending only infrequent feedback.

Figure 5 shows the maximum MEHR versus the number of transmit nodes M. It is observed that the maximum MEHR always lies between the coherent power level and the non-coherent power level and monotonically increases with respect to the the number of transmit nodes. Effectively, although the MEHR is increasing with M, the increasing cost of feedback results in less coherency for large distributed transmit arrays.

VI. Conclusion

This paper considers the combination of feedback-based distributed transmit beamforming and wireless power transfer.

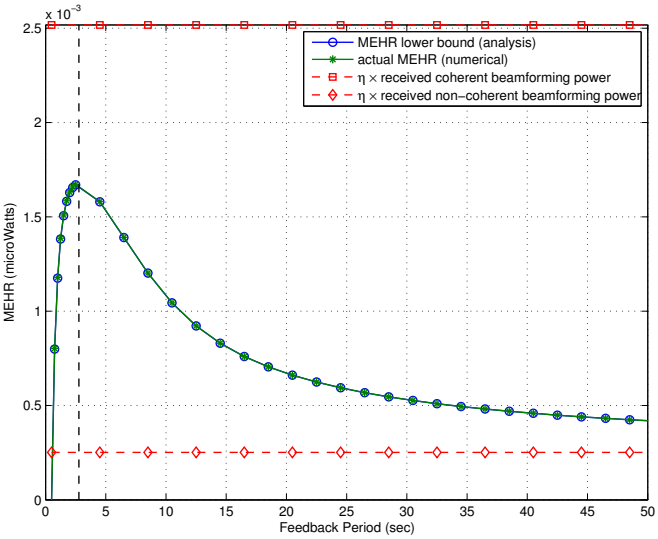

Fig. 3. MEHR versus feedback rate for $M = 10$ transmit nodes system.

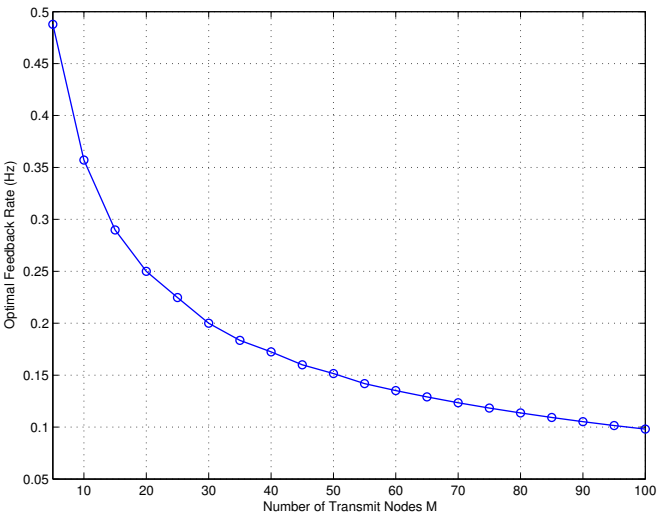

Fig. 4. Optimal feedback rate versus number of transmit nodes.

Analysis of a lower bound on the MEHR shows that there always exists a unique optimal feedback rate to maximize the net energy harvested per unit time. Numerical results verify the analysis and demonstrate the potential for combining distributed transmit beamforming and wireless power transfer.

Future work will consider the effects of feedback latency, systems with per-node power constraints, and systems with forward/reverse link reciprocity.

Appendix

This appendix provides a proof to Theorem 1.

Proof: From (1) and (15), the MEHR can be written as

$$\text{MEHR} = \frac{1}{T_f}\left(\eta\int_{kT_f}^{kT_f+T_b}\check{J}(T_f,t)\,dt - E_f\right).$$

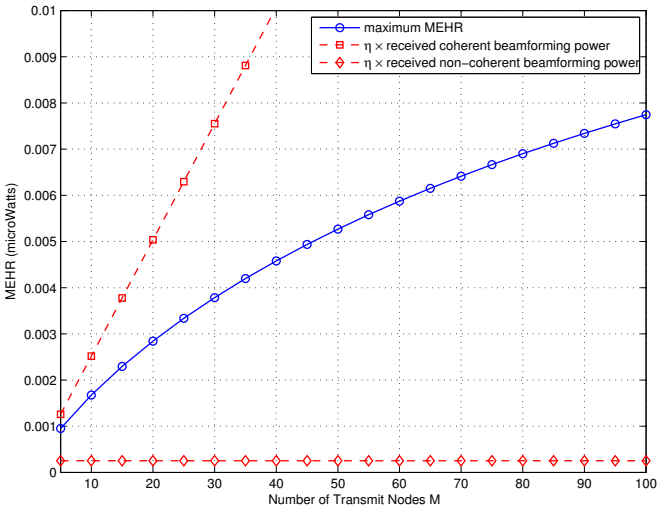

Fig. 5. Maximum MEHR versus number of transmit nodes.

A necessary condition of the optimality of $T_f^\star$ is the first derivative of MEHR with respect to T_f should be zero at $T_f^\star$. From (15), note that

$$\int_{kT_f}^{kT_f+T_b} \check{J}(T_f,t)\,dt = g^2 \int_{kT_f}^{kT_f+T_b} Ce^{-Q(t-kT_f)}+1\,dt$$
$$= g^2 \int_0^{T_b} Ce^{-Q(t)}+1\,dt.$$

Recalling that $T_b = T_f - T_m$, this result along with the Leibniz integral rule [19] implies

$$\frac{\partial}{\partial T_f}\int_{kT_f}^{kT_f+T_b} \check{J}(T_f,t)\,dt = \frac{\partial}{\partial T_f}\left(g^2\int_0^{T_f-T_m} Ce^{-Q(t)}+1\,dt\right)$$
$$= g^2\left(Ce^{-Q(T_b)}+1\right).$$

Hence, we can write

$$\frac{\partial \mathsf{MEHR}}{\partial T_f} = -\frac{\eta g^2}{T_f^2}\left(C\int_0^{T_b} e^{-Q(t)}\,dt + T_b - \frac{E_f}{\eta g^2}\right)$$
$$+\frac{\eta g^2}{T_f}\left(Ce^{-Q(T_b)}+1\right)$$
$$= \frac{\eta g^2}{T_f^2}\left(T_m + \frac{E_f}{\eta g^2} - CF(T_b)\right)$$

where the final equality uses (16) and the fact that $T_f - T_b = T_m$. Since $\eta \in (0,1)$ and $T_f > 0$, this result implies

$$\frac{\partial \mathsf{MEHR}}{\partial T_f} = 0 \quad \text{iff} \quad F(T_b) = \frac{1}{C}\left(T_m + \frac{E_f}{\eta g^2}\right).$$

which provides us the equation in (18). In light of the monotonicity of F, a solution to (18) exists if and only if

$$\frac{1}{C}\left(T_m + \frac{E_f}{\eta g^2}\right) \le \lim_{T_b\to\infty} F(T_b) = \lim_{T_b\to\infty}\int_0^{T_b} e^{-Q(t)}\,dt$$

since $\lim_{T_b\to\infty} e^{-Q(T_b)}T_f = 0$. Moreover, note that

$$\begin{cases} \frac{\partial \mathsf{MEHR}}{\partial T_f} > 0 & ,\forall T_f < T_f^\star \\ \frac{\partial \mathsf{MEHR}}{\partial T_f} < 0 & ,\forall T_f > T_f^\star \end{cases}$$

due to the monotonicity of F, where $T_f^\star = T_b^\star + T_m$ and $T_b^\star$ satisfies (18). Hence, the $T_b^\star$ satisfying (18) is the unique optimal solution of the MEHR maximization problem. ■

REFERENCES

[1] R. Mudumbai, G. Barriac, and U. Madhow, "On the feasibility of distributed beamforming in wireless networks," *Wireless Communications, IEEE Transactions on*, vol. 6, no. 5, pp. 1754–1763, May 2007.

[2] R. Mudumbai, D. Brown, U. Madhow, and H. Poor, "Distributed transmit beamforming: challenges and recent progress," *Communications Magazine, IEEE*, vol. 47, no. 2, pp. 102–110, February 2009.

[3] R. Preuss and D.R. Brown III, "Retrodirective distributed transmit beamforming with two-way source synchronization," in *Information Sciences and Systems (CISS), 2010 44th Annual Conference on*, March 2010, pp. 1–6.

[4] ——, "Two-way synchronization for coordinated multicell retrodirective downlink beamforming," *Signal Processing, IEEE Transactions on*, vol. 59, no. 11, pp. 5415–5427, Nov 2011.

[5] D.R. Brown III, P. Bidigare, and U. Madhow, "Receiver-coordinated distributed transmit beamforming with kinematic tracking," in *Acoustics, Speech and Signal Processing (ICASSP), 2012 IEEE International Conference on*, March 2012, pp. 5209–5212.

[6] D.R. Brown III and R. David, "Receiver-coordinated distributed transmit nullforming with local and unified tracking," in *Acoustics, Speech and Signal Processing (ICASSP), 2014 IEEE International Conference on*, May 2014, pp. 1160–1164.

[7] P. Bidigare, M. Oyarzun, D. Raeman, D. Cousins, D. Chang, R. O'Donnell, and D.R. Brown III, "Implementation and demonstration of receiver-coordinated distributed transmit beamforming across an ad-hoc radio network," in *Proc. of the 46th Asilomar Conf. on Signals, Systems, and Computers*, Pacific Grove, CA, November 4-7 2012, pp. 222–226.

[8] D. Scherber, R. O'Donnell, M. Rebholz, M. Oyarzun, C. Obranovich, W. Kulp, P. Bidigare, and D.R. Brown III, "Coherent distributed techniques for tactical radio networks: Enabling long range communications with reduced size, weight, power and cost," in *MILCOM 2013*, San Deigo, CA, November 18-20 2013.

[9] V. Liu, A. Parks, V. Talla, S. Gollakota, D. Wetherall, and J. R. Smith, "Ambient backscatter: Wireless communication out of thin air," in *Proceedings of the ACM SIGCOMM 2013 Conference on SIGCOMM*, 2013, pp. 39–50.

[10] K. Finkenzeller, *RFID Handbook: Fundamentals and Applications in Contactless Smart Cards and Identification*, 2003.

[11] J. R. Smith, *Wirelessly Powered Sensor Networks and Computational RFID*. Springer, 2013.

[12] L. Varshney, "Transporting information and energy simultaneously," in *Information Theory, 2008. ISIT 2008. IEEE International Symposium on*, July 2008, pp. 1612–1616.

[13] X. Zhou, R. Zhang, and C. K. Ho, "Wireless information and power transfer: Architecture design and rate-energy tradeoff," *Communications, IEEE Transactions on*, vol. 61, no. 11, pp. 4754–4767, November 2013.

[14] L. Liu, R. Zhang, and K.-C. Chua, "Wireless information and power transfer: A dynamic power splitting approach," *Communications, IEEE Transactions on*, vol. 61, no. 9, pp. 3990–4001, September 2013.

[15] P. Grover and A. Sahai, "Shannon meets tesla: Wireless information and power transfer," in *Information Theory Proceedings (ISIT), 2010 IEEE International Symposium on*, June 2010, pp. 2363–2367.

[16] L. Galleani, "A tutorial on the 2-state model of the atomic clock noise," *Metrologia*, vol. 45, no. 6, pp. S175–S182, Dec. 2008.

[17] Y. Bar-Shalom, X. Rong Li, and T. Kirubarajan, *Estimation with Applicatins to Tracking and Navigation*. John Wiley and Sons, 2001.

[18] "Rakon RFPO45 crystal oscillator datasheet," 2009. [Online]. Available: http://www.rakon.com/Products/Public/Documents/ Specifications/RFPO45.pdf

[19] H. Flanders, "Differentiation under the integral sign," *The American Mathematical Monthly*, vol. 80, no. 6, pp. 615–627, 1973.